PCCP

Accepted Manuscript

ROYAL SOCIETY OF CHEMISTRY

www.rsc.org/pccp

Tuning electronic and magnetic properties of GaN nanosheets by surface modifications and the nanosheet thickness

Meixia Xiao[*,a], Tingzhen Yao[a], Zhimin Ao[b], Peng Wei[a], Danghui Wang[a], and Haiyang Song[a]

[a]School of Materials Science and Engineering, Xi'an Shiyou University, Xi'an 710065, People's Republic of China

[b]Centre for Clean Energy Technology, School of Chemistry and Forensic Science, University of Technology Sydney, PO Box 123, Broadway, Sydney, NSW 2007, Australia

Abstract

Density-functional theory calculations are performed to investigate the effects of surface modifications and the thickness on the electronic and magnetic properties of gallium nitride (GaN) nanosheets (NSs). Different from bare GaN NSs terminating with polar surfaces, the systems with hydrogenated Ga (H–GaN), fluorinated Ga (F–GaN), and chlorinated Ga (Cl–GaN) preserve the initial wurtzite structures, and exhibit ferromagnetic states. The above three different decorations on Ga atoms are more energetically favorable for thicker GaN NSs. Moreover, as the thickness increases, H–GaN and F–GaN NSs have respectively semiconductor–to–metal and half-metal–to–metal transition, while Cl–GaN NSs remain fully-metallic. The predicted diverse and tunable electronic and magnetic properties highlight the potential of GaN NSs for novel electronic and spintronic nanodevices.

[*]Corresponding authors. Email: mxxiao@xsyu.edu.cn

Introduction

Nowadays, low-dimensional semiconductor materials are very interesting topics in materials science community due to their highly potential applications in nanodevices, such as new electronic, optical, electrochemical, and electromechanical devices.[1,2] More interestingly, a material, exhibiting metallic behavior for electron spins with one orientation but insulating for the spins with the opposite orientation, is highly desirable in spintronic nanodevices.[3] In addition, magnetism of the two-dimensional (2D) nanosheets (NSs) has attracted more and more interests recently, since the NSs offer unique electronic and magnetic properties that can be efficiently modulated by surface modifications and the thickness.[4-8]

Gallium nitride (GaN) is a large band gap semiconductor with extraordinary physical properties, which has attracted increasing attention (from bulk to nanoscale) due to its excellent performance in optics, electronics, and spintronics.[9] Different types of GaN nanomaterials, such as nanotubes,[10] nanobelts,[11] and nanoribbons,[12,13] were also synthesized. It was found that the III–V compounds, such as AlN and GaN, had stable monolayer honeycomb structure.[14] In particular, a recent theoretical study predicted that a GaN NS transforms into a 2D graphitic structure when it is in the form of an ultrathin film.[15] Due to 2D NSs having higher surface–to–volume ratio compared to bulk materials, surface modification plays an important role in determining its properties, paving a way to tune the band gaps and magnetic properties of the semiconductor NSs. Molecules and atoms adsorbed on graphene surfaces are known to serve as local doping sites that significantly alter graphene's electronic properties.[16-18] For example, N-doped graphene with two H atoms adsorbed has an indirect band gap of around 3 eV in the band structure,[19] semihydrogenated graphene becomes a ferromagnetic (FM) semiconductor with a small indirect gap,[20]

and zigzag–edged triangular graphene nanoflakes embedded in graphane exhibit a FM ground state.[21] Monolayer BN NSs can be FM, antiferromagnetic (AFM), or magnetically degenerate depending on different surface modifications.[22] FM and metallic properties of the one–bilayer GaN NSs can be also achieved by semihydrogenation.[23] Meanwhile, the versatility in surface modifications and the thickness of new materials, such as ZnO,[24,25] AlN,[26] and Co_9Se_8[27] NSs, allow us to envision new devices with semiconductor, half-metal, ormetal features. For example, Zhu *et al.* reported that the band gaps with 2.5, 1.7, 1.1, and 0.6 eV are largely dependent on the size for the first, second, third, and fourth nanoarray graphene-based sheets.[28]

All above works offer interesting opportunities to achieve tunable electronic and magnetic properties of the NSs by controlling different surface modifications and the NS thickness. Therefore, it would be very interesting to investigate the effects of decoration with H, F, or Cl atoms and the NS thickness on the electronic and magnetic properties. Both bare and fully hydrogenated GaN NSs have been found that they are nonmagnetic (NM) at the ground states and have a semiconductor–to–metal transition when the thickness exceeds a certain critical value.[29] In this paper, we use density-functional theory (DFT) calculations to explore the possibility of tuning electronic and magnetic properties of semihydrogenated, semifluorinated, and semichlorinated GaN NSs with the increasing thickness. These results will provide guidance to future experiments and fully exploit these materials for innovative electronic and spintronic nanodevice applications.

Computational methods

Our calculations are based on spin-polarized density functional theory using the DMol^3 code,[30,31] with the generalized gradient approximation (GGA) of

Perdew-Burke-Ernzerhof (PBE) as the exchange-correlation functional.[32] For the geometric, electronic, and magnetic calculations, the supercells consisting of fourfold unit cells of GaN NSs are used with vacuum spaces of 15 Å above to avoid the interactions between neighboring cells. The atoms are relaxed without any constraints. The DFT semicore pseudopots is implemented for relativistic effects, which replaces core electrons by effective potentials for Ga and In elements;[33] all-electron is used for the core treatment for N, H, F, and Cl elements.[34] In addition, Double Numerical plus Polarization (DNP) atomic orbitals are chosen as the basis sets.[30] The Brillouin zone integration is set to be 9×9×1 *k*-points for the geometry optimizations and 17×17×1 k-points for the static total energy calculations.[35] We use smearing techniques to achieve self-consistent field convergence with a smearing value of 0.001 Ha (1 Ha = 27.2114 eV).[36] The convergence tolerances of energy, maximum force and the maximum displacement are 1.0×10^{-5} Ha, 0.002 Ha/Å, and 0.005 Å, respectively.

The lattice constants of the calculated bulk GaN are $a = b = 3.182$ Å, $c = 5.180$ Å with an internal coordinate of $u = 0.377$. The average Ga–N bond length is 1.951 Å, and band gap of bulk GaN is 2.58 eV, consistent with previous GGA calculations of 2.58 eV, although smaller than the experimental value (3.45 eV).[37] Although the hybrid functionals, such as HSE,[38] PBE0,[39] or B3LYP,[40,41] represent the stated-of-the-art approach to accurately evaluate the band structures, the hybrid functionals are very time consuming and it would quickly become prohibitively expensive as the system size grows. In this work, it is only required to predict the reasonable trends for changes of band gaps in the GaN NSs. Thus, it is considered that DFT–GGA based calculations should be enough as long as all the calculations using the same settings.[42] All GaN NSs are constructed from the bulk wurtzite structures and terminated with polar (0001) surfaces. We study the semihydrogenated,

semifluorinated, and semichlorinated GaN NSs with the thickness ranging from 2 to 5 bilayers (a bilayer is composed of two closely adjacent layers, one for Ga layer and the other for N layer, e.g., the GaN NS in Fig. 1 contains two bilayers).

Results and discussion

The accuracy of our calculation procedure is tested using bare GaN NSs. The optimized structures of GaN NSs with different bilayer-thickness are labeled as *n*–GaN NSs, where *n* represents the number of bilayers in thickness along the (0001) axial direction. We perform the structural relaxations of bare GaN NSs with the bilayer numbers ranging from 2 to 5. The bare *n*–GaN NSs ($2 \leq n \leq 5$) transform from the initial wurtzite configurations to the flat graphitic structures, an examples of $n = 2$ for before and after geometry optimization are shown in Figs. 1(a) and 1(b), respectively. Meanwhile, all the graphitic GaN NSs are semiconductors with indirect band gaps, and the band gap decreases smoothly with the increasing thickness due to the intrinsic surface states arising from the unsaturated dangling bonds on the polar surface.[29] In addition, spin–polarized calculations show that the bare GaN NSs are NM semiconductors. The results are consistent with previous predictions.[15,29,43]

Similar to BN and ZnO NSs,[22,44] Ga and N sites in GaN NSs are chemically nonequivalent, and semidecoration can be achieved by merely saturating either all the Ga atoms or all the N atoms. We first study hydrogenation, fluorination, and chlorination on Ga atoms for GaN NSs with different bilayer numbers (labeled as *n*–M–GaN). Their relaxed atomic configurations of 2–M–GaN NSs from side view are shown in Fig. 1(c), whose top views of three magnetic coupling configurations between N atoms: FM coupling, AFM coupling, and NM coupling are given in Fig. 1(d). The geometric optimization shows that the GaN surface becomes less distorted, and all M atoms are adsorbed on Ga atoms with M–Ga bonds arranged

perpendicularly to GaN plane. The formation of M–Ga bond generates one hole per unit cell and hence one unpaired spin at each surface N atom. In order to study the preferred coupling of these magnetic moments of surface N atoms in *n*–M–GaN NSs, the total energies of the above three magnetic configurations between N atoms are calculated. Table 1 lists the relative energies of semidecorated GaN NSs with NM, FM, and AFM states, respectively. The calculated FM states of M–GaN NSs ($2 \leq n \leq 5$) are energetically lower than those of the AFM and NM states, indicating that these M–GaN NSs exhibit FM states. Our results are consistent with the previous predictions that the FM state prefers monolayer H–GaN NS.[4,23]

The results of *n*–H–GaN NSs ($2 \leq n \leq 5$) are summarized in following. In all cases, spin polarization is evident in the band structure and PDOS as shown in Fig. 2. This is because hydrogenation on Ga atoms forms strong Ga–H bonds and leaves the dangling bonds of surface N atoms spin unpaired. The origin of the magnetic behavior is further investigated by plotting the spin density distribution. It is confirmed that the induced magnetism is attributed by the every spin unpaired N atom that carries a magnetic moment of about 0.72, 0.65, 0.63, and 0.62 μ_B per unit cell for two, three, four, and five bilayers, respectively. Obviously, the emergent spin polarization is not restricted to the surface N atoms but instead is delocalized uniformly on N atoms in the entire system, leading to a corresponding net magnetic moment of all atoms with approximately 0.93, 0.84, 0.77, and 0.72 μ_B, respectively per unit cell. The induced magnetism is attributed primarily by the undecorated N atoms, with only a little contribution from other atoms. More careful examination of the band structures of *n*–M–GaN NSs reveals appealing properties associated with this novel system. As described in Figs. 2(a) and 2(b), the 2–H–GaN NS behaves as a FM semiconductor with band gaps of 4.01 and 0.08 eV in the spin-up and spin-down states, respectively.

The absorption of H atom on Ga atoms introduces a low acceptor level located slightly above the valence band maximum (VBM), which is spin-polarized with only one spin channel completely occupied, resulting in hole-doping *p*-type semiconductivity. The van der Waals (vdW) interactions open the band gaps of silicene and graphene in hybrid layered materials,[45] for example silicene/silicon NSs,[46] graphene/BN,[47] and silicene/Ag NSs,[48] and allow quantitative treatment of both weakly and strongly adsorbed molecules on metal surfaces,[49] such as benzene/metal.[50-52] We utilize DFT–D functional with Grimme method, which considers vdW interactions, to calculate the band structure of 2–H–GaN NS. It is found that 2–H–GaN NS remains a FM semiconductor with 3.99 eV in the spin-up state and 0.06 eV in the spin-down state. The DFT calculations slightly overestimate the band gaps with 0.02 eV in spin-up and spin-down states, respectively. The results imply that DFT can give a qualitative trend of the electronic and magnetic properties of semidecorated GaN NSs. The 3–H–GaN NS remains the magnetic semiconductor with the direct band gaps of 3.55 and 0.03 eV in the spin-up and spin-down states, respectively. Interestingly, when the bilayer number further increases to four or even five, both the spin-up and spin-down states become metallic, indicating that the semihydrogenated multilayer NSs are all metals with strong spin polarization, as seen in Figs. 2(c) and 2(d). The results are different from those of semihydrogenated *n*–H–AlN NSs that they ($2 \leq n \leq 5$) show half-metallic character with an indirect band gap in the spin-up channel.[26] The reason can be explained through bond lengths of Ga–H bonds. With increasing thickness of GaN NSs, the drastically decreasing Ga–H bond length indicates the reinforcement of the bonding hybridization effect, which broadens both occupied spin-up and unoccupied spin-down channels. The results make Fermi level lie in the H-induced bands and induce the metallic behaviors.

With fluorination on Ga sites, *n*–F–GaN ($2 \leq n \leq 4$) NSs always exhibit half-metallic behavior. For 2–F–GaN NS, the spin-up state behaves as a semiconductor with a direct band gap of 3.79 eV, whereas the spin-down state shows metallic character in Figs. 3(a)–3(b) by DFT calculations, while the half-metallic behavior (3.78 eV in spin-up state) is obtained by DFT–D calculations. A direct band gap in the spin-up state reduces to 3.42, and 3.10 eV, and the spin-down state remains metallicity, as the bilayer number increases to three and four. However, when the thickness reaches to five bilayers, both spin-up and spin-down channels of the 5–F–GaN NS are broadened because of the hybridization effect, which lifts the VBM and the NS exhibits a metallic behavior [Figs. 3(c)–3(d)]. As shown in the PDOS, the spin-polarized magnetization still mainly comes from the 2*p* orbital of the undecorated N atoms. The calculated magnetic moments are 0.98, 0.85, 0.78, and 0.76 μ_B per unit cell of F–GaN NSs with two, three, four, and five bilayers, respectively. Meanwhile, the every undecorated N atom in F–GaN NSs possesses slightly more magnetic moment compared with H–GaN NSs and the corresponding values are about 0.72, 0.66, 0.64, and 0.63 μ_B, respectively. This is easily understandable that the semifluorination on Ga atoms with stronger F–Ga bonds induces the dangling bonds on unpaired N atoms, which exhibit much more spin density compared with the effects of the semihydrogenation on Ga atoms. The undecorated N atoms receive fewer electrons in F–GaN NSs than those in H–GaN NSs due to the stronger electronegativity of F element. Moreover, the magnetic moment per unpaired N atom decreases as the bilayer number increases. The main reason is that the undecorated atoms receive more electrons with the increasing bilayer number due to the interlayer interactions, suggesting the strong spin density.

However, the semichlorination on Ga atoms induces the *n*–Cl–GaN NSs being

practically FM metal with the bilayer number ranging from 2 to 5. Both DFT and DFT–D calculations show the 2–Cl–GaN NSs are metallic. Fig.4 presents that the results of the band structures and PDOS, where the spin-up and spin-down states cross the Fermi level due to chlorine-derived hybridization effect. The spin-polarized magnetization has a significant weight distributed on the 2*p* orbital of the undecorated N atom, and the calculated magnetic moments are 0.58, 0.60, 0.61, and 0.63 μ_B per unit cell by increasing the thickness, respectively. This remarkable phenomenon different from those of H–GaN and F–GaN NSs can be further scrutinized by analyzing the nature of Ga–M bonds. Noticeably, the Ga–Cl bond length decreases drastically as the thickness increases, which indicates the reinforcement of Ga–Cl bonds.

The results above demonstrate theoretically that the electronic and magnetic properties of GaN NSs can be tuned through decorating H, Cl and F atoms on Ga in GaN NSs using different elements. It is shown that, by decorating its surface with H, F, Cl atoms, 2–H–GaN, 2–F–GaN, and 2–Cl–GaN NSs in FM states are predicated to be semiconductor, half-metal, and metal, respectively. Meanwhile, the magnetic moment of undecorated N atom for *n*–H–GaN and *n*–F–GaN NSs decreases as the NSs thickness increases, however, that for *n*–Cl–GaN NSs increases. The electronic and magnetic properties can be determined by the combination of two interactions:[53] (a) through-bond interaction and (b) *p*–*p* direct interaction of surface N atoms. Through-bond interaction indicates that an atom with spin-up (spin-down) density induces a spin-down (spin-up) density on the adjacent atom directly bonded to it, while the *p*–*p* direct interaction suggests that an atom with spin-up (spin-down) density induces a spin-down (spin-up) density on the nearest-neighboring atom of the same element directly without mediated by another different atom. Although the

effects of through-bond and *p*–*p* direct interactions are the same thing from the viewpoint of bonding theory, the through-bond spin polarization of N atom is an indirect interaction mediated by the neighboring Ga atom, while *p*–*p* direct spin polarization is a direct interaction through space. Two interactions may be available together. Based on this mechanism, we can also understand the evolution of the electronic and magnetic properties of the three *n*–M–GaN NSs. The results show that for the three *n*–M–GaN NSs in FM states, the distance $d_{N–N}$ between two neighboring N atoms is about 3.182 Å due to the same GaN NSs. However, the bond length $d_{N–Ga}$ between surface N and the neighboring Ga atoms for H–GaN NSs is the largest, while that for Cl–GaN NSs is the smallest, as the bilayer number is the same. This is responsible for the relatively weakest and strongest effects of semihydrogenation and semichlorination on GaN NSs, respectively. The results explain the reason that 2–H–GaN, 2–F–GaN and 2–Cl–GaN NSs exhibit semiconductor, half-metal, and metal, respectively. In addition, the bond length $d_{N–Ga}$ between undecorated N and neighboring Ga atoms for *n*–H–GaN and *n*–F–GaN NSs decreases, while that for *n*–Cl–GaN increases, as the thickness increases. Evidently, the facts also indicate that the interaction between the magnetic moments is mainly determined by the effect of through-bond spin polarization, resulting in the different tendency of the magnetic moment of the unpaired N atoms. More importantly, this mechanism is hold by the electronic and magnetic properties of semifluorinated 2D systems, such as semifluorinated bilayer of BN, GaN and graphene.[53]

After considering the case of M on Ga atoms, we discuss the electronic and magnetic properties of *n*–GaN–M NSs, where M atoms bind with N atoms. In the reported 1–BN–H NSs with AFM properties,[22] H atoms act as electron donors, which reduces the charge transfer from B to N, leaving 2*p* electron spin in B site unpaired.

However, as listed in table 1, the relative energies of the GaN NSs with NM or AFM states compared with FM states are close to zero. Thus the *n*–GaN–M NSs with the semihydrogenation, semifliorination, and semichlorination on N sites ($2 \leq n \leq 5$) exhibit practically NM metallicity. The similar metallic characteristics have been discovered in single GaN NSs with hydrogenated N atoms.[23] The reason is that the electronegativity of Ga ions is smaller than that of B ions, so that the released 2*p* electron from N ions cannot be confined in 4*p* orbital of Ga. For simplicity, the band structure and PDOS of the 2–GaN–F NS are provided in Fig. 5 as an example. The results show that the 2–GaN–F NS turns metallic with bands crossing the Fermi level due to the hybridization effects of fluorination on N atoms, and the symmetrical spin-up and spin-down channels of the PDOS imply the 2–GaN–F with an NM system.

Therefore, the semidecoration on Ga atoms rather on N atoms is effective for tuning the electronic and magnetic properties of GaN NSs. To determine the structural stability of the *n*–M–GaN NSs, the calculated binding energies of these systems E_b can be expressed as $E_b = (E_{M-GaN} - E_{GaN} - n_M E_M)/n_M$, where E_{M-GaN} and E_{GaN} are the total energies of the GaN NSs with and without semidecoration, and E_M is the energy of the single H, F, or Cl atom. n_M is the number of M atoms. A system with smaller binding energies E_b value is more favorable. Fig. 6 shows the binding energies E_b of the different semidecorated *n*–M–GaN and *n*–GaN–M NSs as a function of bilayer number *n*. The 2–H–GaN, 2–F–GaN, and 2–Cl–GaN NSs have binding energies E_b of –1.10, –3.03, and –1.82 eV based on DFT calculation, which are slightly overestimated compared to the DFT–D results of –1.20, –3.23, and –1.99 eV. The agreement between DFT and DFT–D results indicates that the DFT calculation is accurate to give a stable adsorption state. For the same bilayer number, the

semifluorination on the Ga atoms induce the lowest binding energies E_b of the GaN NSs among three semidecorated Ga atoms, while the semihydrogenation on the N atoms lead to the lowest E_b among three semidecorated N atoms. It is noted that the binding energies E_b progressively decrease with increasing the number of bilayer number n, indicating that functionalization are preferred on thicker GaN NSs.

Conclusion

In summary, we have systematically investigated the electronic and magnetic properties of semidecorated GaN NSs with increasing bilayer number. We predict that n–M–GaN NSs ($2 \leq n \leq 5$) with hydrogenated, fluorinated, and chlorinated Ga atoms exhibit FM states, and the thicker M–GaN NSs are more favorable energetically. H–GaN and F–GaN NSs have a transition from semiconductor and half-metal into metal, while Cl–GaN NSs keep metallic character, as the thickness increases, respectively. However, decoration on N atoms results in practically NM metallicity in GaN NSs. Thus, the intriguing and diverse transformation in electronic and magnetic properties of the novel GaN NSs remarkably depend on surface modifications with H, F, and Cl atoms and the NS thickness. Our results predict that effectively controlling surface modifications and thickness is an effective way to modulate the properties of GaN NSs, and that a transition among semiconductor or metal or half-metal (the change of magnetic moment) can be achieved. These diverse properties are of fundamental significance, which opens up exciting opportunities for the design of electronic and novel spintronic devices.

Acknowledgements

The authors acknowledge the support by Scientific Research Program Funded by Shaanxi Provincial Education Department (2013JK0894), the Program for New Century Excellent Talent in University of Ministry of Education of China (Grant No.

NCET-12-1046), Provincial College Students' Training Programs for Innovation and Entrepreneurship of Shaanxi province (1205), and Youth Science and Technology Innovation Fund Project at the Xi'an Shiyou University (2012BS004). This research is supported by the National Computational Infrastructure (NCI) through the merit allocation scheme and used NCI resources and facilities in Canberra, Australia.

References

1 Y. Zhang, Y. W. Tan, H. L. Stormer and P. Kim, *Nature*, 2005, **438**, 201-204.

2 A. S. Barnard, *J. Mater. Chem.*, 2006, **16**, 813-815.

3 A. Lopez-Bezanilla, P. Ganesh, P. C. Kent and B. Sumpter, *Nano Res.*, 2014, **7**, 63-70.

4 Y. Ma, Y. Dai, M. Guo, C. Niu, L. Yu and B. Huang, *Appl. Surf. Sci.*, 2011, **257**, 7845-7850.

5 Y. F. Zhu, Q. Q. Dai, M. Zhao and Q. Jiang, *Sci. Rep*., 2013, **3**, 1524.

6 J. T. Tanskanen, M. Linnolahti, A. J. Karttunen and T. A. Pakkanen, *J. Phys. Chem. C*, 2008, **113**, 229-234.

7 M. Topsakal, E. Aktürk and S. Ciraci, *Phys. Rev. B*, 2009, **79**, 115442.

8 K. M. Wong, S. M. Alay-e-Abbas, A. Shaukat, Y. Fang and Y. Lei, *J. Appl. Phys.*, 2013, **113**, 014304.

9 H. Morkoc, S. Strite, G. B. Gao, M. E. Lin, B. Sverdlov and M. Burns, *J. Appl. Phys*., 1994, 76, 1363-1398.

10 J. Goldberger, R. He, Y. Zhang, S. Lee, H. Yan, H.-J. Choi and P. Yang, *Nature*, 2003, **422**, 599-602.

11 S. Y. Bae, H. W. Seo, J. Park, H. Yang and S. A. Song, *Chem. Phys. Lett.*, 2002, **365**, 525-529.

12 L. Yang, X. Zhang, R. Huang, G. Zhang and X. An, *Solid State Commun.*, 2004, **130**, 769-772.

13 X. Xiang, C. Cao, F. Huang, R. Lv and H. Zhu, *J. Cryst. Growth*, 2004, **263**, 25-29.

14 H. Şahin, S. Cahangirov, M. Topsakal, E. Bekaroglu, E. Akturk, R. T. Senger and S. Ciraci, *Phys. Rev. B*, 2009, **80**, 155453.

15 C. L. Freeman, F. Claeyssens, N. L. Allan and J. H. Harding, *Phys. Rev. Lett.*, 2006, **96**, 066102.

16 Z. M. Ao, S. Li and Q. Jiang, *Solid State Commun.*, 2010, **150**, 680-683.

17 M. Jaiswal, C. H. Yi Xuan Lim, Q. Bao, C. T. Toh, K. P. Loh and B. Özyilmaz, *ACS Nano*, 2011, **5**, 888-896.

18 W. Gao, J. E. Mueller, J. Anton, Q. Jiang and T. Jacob, *Angew. Chem. Int. Ed.*, 2013, **52**, 14237-14241.

19 Z. M. Ao and F. M. Peeters, *J. Phys. Chem. C*, 2010, **114**, 14503-14509.

20 J. Zhou, Q. Wang, Q. Sun, X. S. Chen, Y. Kawazoe and P. Jena, *Nano Lett.*, 2009, **9**, 3867-3870.

21 Q. Q. Dai, Y. F. Zhu and Q. Jiang, *Phys. Chem. Chem. Phys.*, 2012, **14**, 1253-1261.

22 J. Zhou, Q. Wang, Q. Sun and P. Jena, *Phys. Rev. B*, 2010, **81**, 085442.

23 W.-Z. Xiao, L.-L. Wang, L. Xu, Q. Wan, A.-L. Pan and H.-Q. Deng, *Phys. Status solidi B*, 2011, **248**, 1442-1445.

24 Y. Wang, Y. Ding, J. Ni, S. Shi, C. Li and J. Shi, *Appl. Phys. Lett.*, 2010, *96*, 213117.

25 Q. Chen, J. Wang, L. Zhu, S. Wang and F. Ding, *J. Chem. Phys.*, 2010, **132**, 204703.

26 C.-w. Zhang and F.-b. Zheng, *J. Comput. Chem.*, 2011, **32**, 3122-3128.

27 X. Zhang, J. Zhang, J. Zhao, B. Pan, M. Kong, J. Chen and Y. Xie, *J. Am. Chem. Soc.*, 2012, **134**, 11908-11911.

28 Y. Zhu, N. Zhao, J. Lian and Q. Jiang, *J. Phys. Chem. C*, 2014, **118**, 2385-2390.

29 Q. Tang, Y. Cui, Y. Li, Z. Zhou and Z. Chen, *J. Phys. Chem. C*, 2011, **115**, 1724-1731.

30 B. Delley, *J. Chem. Phys.*, 1990, **92**, 508-517.

31 B. Delley, *J. Chem. Phys.*, 2000, **113**, 7756-7764.

32 J. P. Perdew, K. Burke and M. Ernzerhof, *Phys. Rev. Lett.*, 1996, **77**, 3865.

33 B. Delley, *Phys. Rev. B*, 2002, **66**, 155125.

34 D. D. Koelling and B. N. Hartreermon, *J. Phys. C Solid State Phys.*, 1977, **10**, 3107.

35 H. J. Monkhorst and J. D. Pack, *Phys. Rev. B*, 1976, **13**, 5188.

36 B. Delley, *Modern Density Functional Theory: A Tool for Chemistry; Elsevier Science: Amsterdam*, 1995; Vol. **2**.

37 D. J. Carter, J. D. Gale, B. Delley and C. Stampfl, *Phys. Rev. B*, 2008, **77**, 115349.

38 J. Heyd and G. E. Scuseria, *J. Chem. Phys*., 2004, **121**, 1187-1192.

39 J. Heyd, G. E. Scuseria and M. Ernzerhof, *J. Chem. Phys.*, 2003, **118**, 8207-8215.

40 P. J. Stephens, F. J. Devlin, C. F. Chabalowski and M. J. Frisch, *J. Phys. Chem*., 1994, **98**, 11623-11627.

41 A. D. Becke, *J. Chem. Phys.*, 1993, **98**, 5648-5652.

42 L. Dong, S. K. Yadav, R. Ramprasad and S. P. Alpay, *Appl. Phys. Lett.*, 2010, **96**, 202106.

43 H. Li, J. Dai, J. Li, S. Zhang, J. Zhou, L. Zhang, W. Chu, D. Chen, H. Zhao, J. Yang and Z. Wu, *J. Phys. Chem. C*, 2010, **114**, 11390-11394.

44 Q. Tang, Y. Li, Z. Zhou, Y. Chen and Z. Chen, *ACS Appl. Mater. Inter*., 2010, **2**, 2442-2447.

45 S. Grimme, *J. Comput. Chem.*, 2006, **27**, 1787-1799.

46 S. Li, Y. Wu, W. Liu and Y. Zhao, *Chem. Phys. Lett.*, 2014, **609**, 161-166.

47 X. F. Chen, J. S. Lian and Q. Jiang, *Phys. Rev. B*, 2012, **86**, 125437.

48 Z.-X. Guo and A. Oshiyama, *Phys. Rev. B*, 2014, **89**, 155418.

49 J. van Ruitenbeek, *Nat. Mater*., 2012, **11**, 834-835.

50 W. Liu, S. N. Filimonov, J. Carrasco and A. Tkatchenko, *Nat Commun.*, 2013, 4, 2569.

51 W. Liu, J. Carrasco, B. Santra, A. Michaelides, M. Scheffler and A. Tkatchenko, *Phys. Rev. B*, 2012, **86**, 245405.

52 H. Yildirim, T. Greber and A. Kara, *J. Phys. Chem. C*, 2013, **117**, 20572-20583.

53 Y. Ma, Y. Dai, M. Guo, C. Niu, L. Yu and B. Huang, *Nanoscale*, 2011, **3**, 2301-2306.

Table 1 The relative energies (meV) of semidecorated GaN NSs with NM, FM, and AFM states, respectively. The energy of corresponding FM state of *n*–M–GaN and *n*–GaN–M is set to be 0.

		hydrogenation			fluorination			chlorination		
		NM	FM	AFM	NM	FM	AFM	NM	FM	AFM
n–M–GaN	*n*=2	384	0	49	515	0	79	319	0	46
	n=3	354	0	44	400	0	44	338	0	45
	n=4	353	0	39	383	0	41	347	0	45
	n=5	351	0	39	368	0	38	347	0	44
n–GaN–M	*n*=2	0	0	-4	0	0	-4	0	0	0
	n=3	0	0	-5	0	0	-5	0	0	0
	n=4	0	0	-6	0	0	-6	0	0	0
	n=5	0	0	-6	0	0	-6	0	0	0

Fig. 1 (Color online) Optimized atomic structures of bare two–bilayer (2–GaN) NS (a) before and (b) after geometry optimization, (c) semidecorated two–bilayer (2–M–GaN) NS in side views, and (d) three magnetic coupling states with FM, AFM, and NM states in top views. The large (light pink) and middle (dark blue) spheres represent Ga and N atoms, respectively, while the smallest light blue spheres represent M atoms (H, F or Cl atoms).

Fig. 2 Calculated band structures and partial density of states (PDOS) of (a–b) 2–H–GaN and (c–d) 4–H–GaN NSs in FM states.

Fig. 3 Calculated band structures and partial density of states (PDOS) of (a–b) 2–F–GaN, and (c–d) 5–F–GaN NSs in FM states.

Fig. 4 Calculated (a) band structures and (b) PDOS of 2–Cl–GaN NS in FM state.

Fig. 5 Calculated (a) band structures and (b) PDOS of 2–GaN–F NS.

Fig. 6 Calculated binding energies E_b (in eV) of different GaN NSs with decorated (a) Ga atoms and (b) N atoms, as a function of bilayer number n, respectively.

Fig.1

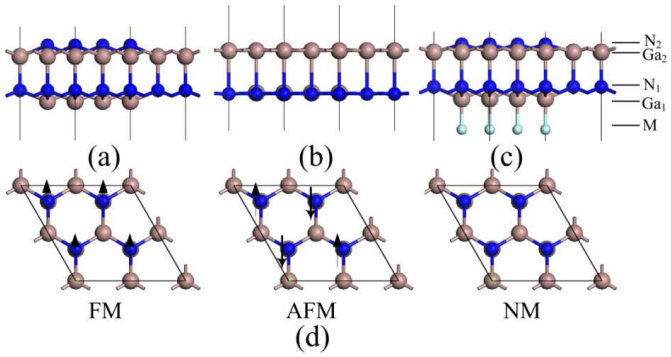

Fig. 2

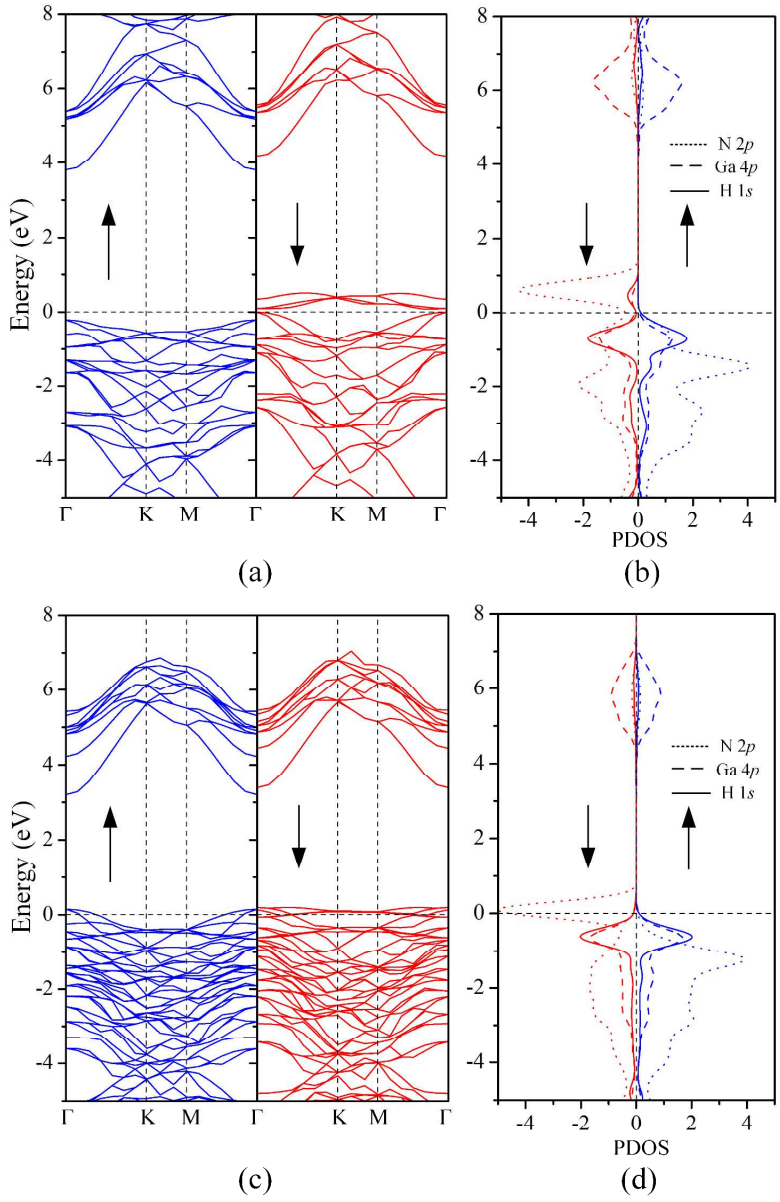

Fig. 3

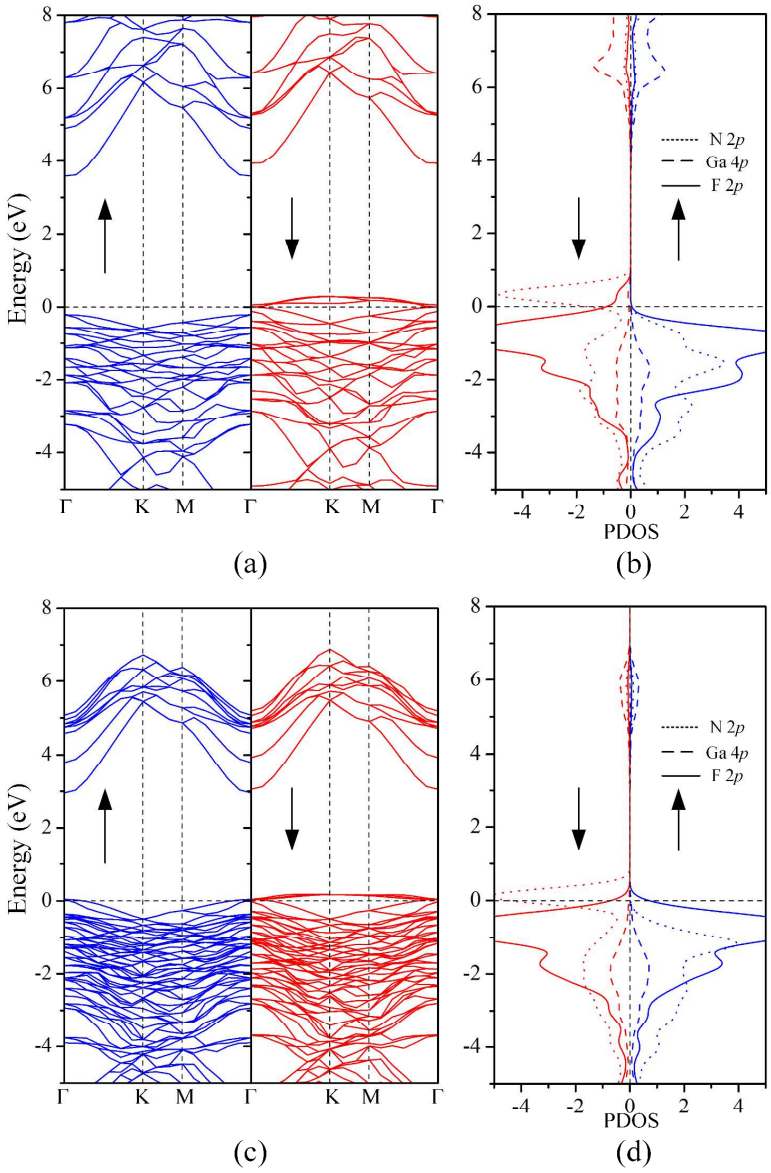

Fig. 4

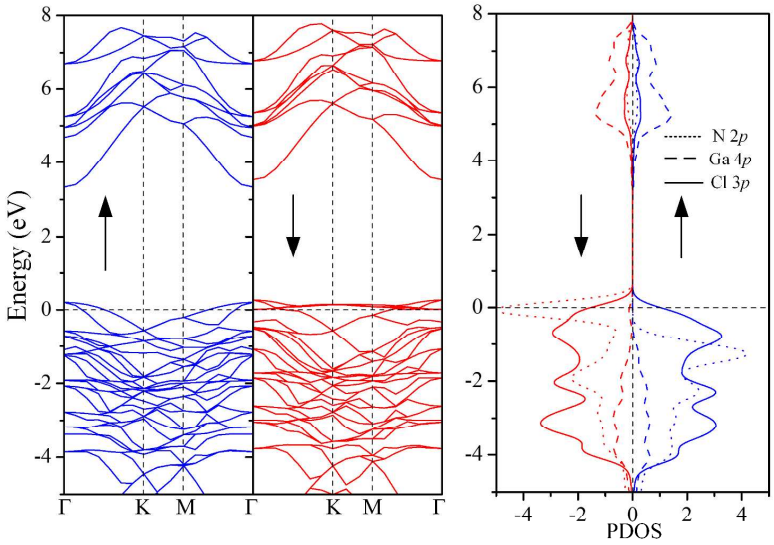

Fig. 5

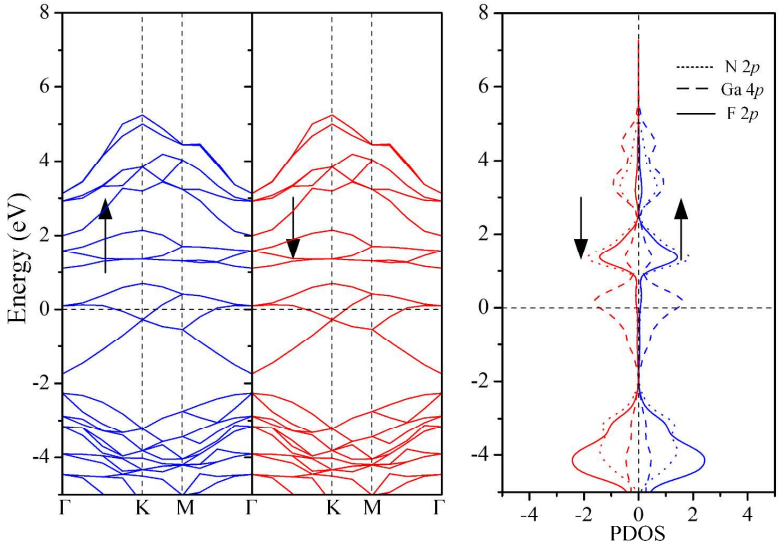

Fig. 6

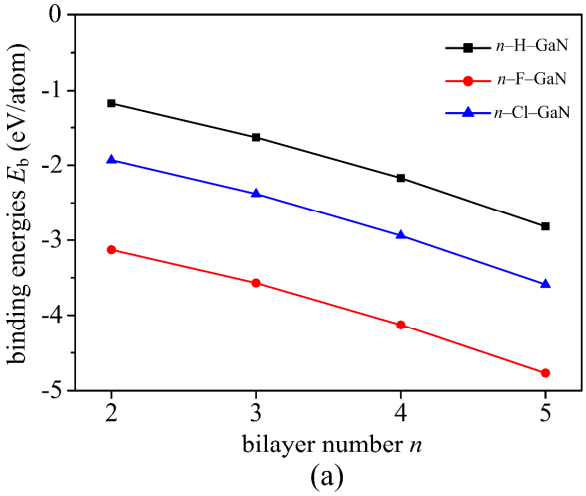

(a)

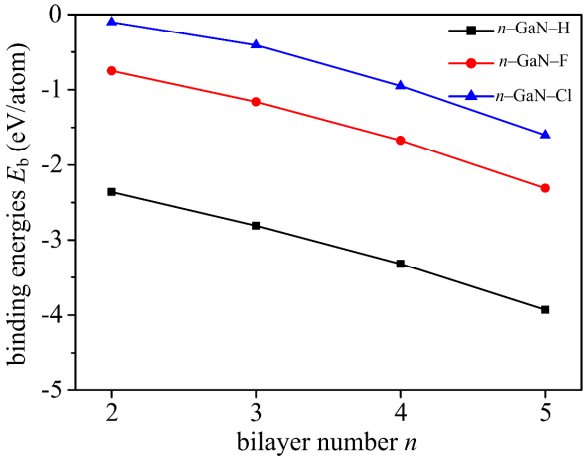

(b)